Pergamon

Geochimica et Cosmochimica Acta, Vol. 63, No. 19/20, pp. 3003–3008, 1999
Copyright © 1999 Elsevier Science Ltd
Printed in the USA. All rights reserved
0016-7037/99 $20.00 + .00

PII S0016-7037(99)00227-6

Effect of hydroxamate siderophores on Fe release and Pb(II) adsorption by goethite

STEPHAN M. KRAEMER,[1,*] SING-FOONG CHEAH,[1] RITA ZAPF,[1,†] JIDE XU,[2] KENNETH N. RAYMOND,[2] and GARRISON SPOSITO[1]

[1]Division of Ecosystem Sciences, University of California, Berkeley, California 94720-3110, USA
[2]Department of Chemistry, University of California, Berkeley, California 94720-1460, USA

(*Received October* 15, 1998; *accepted in revised form April* 29, 1999)

Abstract—Hydroxamate siderophores are biologically-synthesized, Fe(III)-specific ligands which are common in soil environments. In this paper, we report an investigation of their adsorption by the iron oxyhydroxide, goethite; their influence on goethite dissolution kinetics; and their ability to affect Pb(II) adsorption by the goethite surface. The siderophores used were desferrioxamine B (DFO-B), a fungal siderophore, and desferrioxamine D_1, an acetyl derivative of DFO-B (DFO-D1). Siderophore adsorption isotherms yielded maximum surface concentrations of 1.5 (DFO-B) or 3.5 (DFO-D1) μmol/g at pH 6.6, whereas adsorption envelopes showed either cation-like (DFO-B) or ligand-like (DFO-D1) behavior. Above pH 8, the adsorbed concentrations of both siderophores were similar. The dissolution rate of goethite in the presence of 240 μM DFO-B or DFO-D1 was 0.02 or 0.17 μmol/g hr, respectively. Comparison of these results with related literature data on the reactions between goethite and acetohydroxamic acid, a monohydroxamate ligand, suggested that the three hydroxamate groups in DFO-D1 coordinate to Fe(III) surface sites relatively independently. The results also demonstrated a significant depleting effect of 240 μM DFO-B or DFO-D1 on Pb(II) adsorption by goethite at pH $>$ 6.5, but there was no effect of adsorbed Pb(II) on the goethite dissolution rate. *Copyright © 1999 Elsevier Science Ltd*

1. INTRODUCTION

Siderophores are Fe(III)-specific ligands of low relative molecular mass that are synthesized by fungi and bacteria as a response to iron stress (Powell et al., 1982; Telford and Raymond, 1996). Fungi produce mainly trihydroxamate siderophores, a typical example being desferrioxamine B (Powell et al., 1982; Crumbliss, 1991; Albrecht-Gary and Crumbliss, 1998), in which three hydroxamate groups (Fig. 1) contribute to hexadentate ligation of Fe^{3+} in 5 membered rings with an exceptional combination of high specificity and stability (1:1 complex formation constant of 10^{31} (Telford and Raymond, 1996), as compared to 10^{25} for Fe-EDTA). These siderophores are common in soil environments (Powell et al., 1982; Crowley and Gries, 1994). Their soil solution concentrations increase significantly with organic matter content and with proximity to living plant roots (Powell et al., 1982; Crowley et al., 1987).

Watteau and Berthelin (1994) demonstrated the efficacy of trihydroxamate siderophores as promoters of Fe(III)-mineral dissolution by incubating samples of synthetic goethite (α-FeOOH) over a month long period at 24°C with *Suillus granulatus*, an ectomychorrhizal fungus, and with an abiotic 126 (μM solution of desferrioxamine B. Significant quantities of Fe were mobilized by the fungi in close correspondence with their production of siderophores. Goethite was dissolved very rapidly at pH 3 by desferrioxamine B ($<$2 days) at a rate that was about an order of magnitude greater than dissolution at pH 3 promoted by H^+ or by common aliphatic acids. Noting that the Fe solubilized after 28 days accounted for only about 8% of the complexing capacity of the added desferrioxamine B, Watteau and Berthelin (1994) suggested that further research was needed on the accessibility of this siderophore to the goethite surface.

Holmén and Casey (1996; 1998) and Holmén et al. (1997) have explored the mechanisms of hydroxamate-promoted dissolution of goethite in studies utilizing a model compound, acetohydroxamic acid (Fig. 1), which is a small ligand possessing a single hydroxamate functional group. They concluded from dissolution kinetics data, as well as from FTIR spectroscopic measurements, that adsorbed acetohydroxamic acid forms a surface chelate with exposed Fe^{3+} by an associative ligand exchange mechanism (Stumm et al., 1990; Holmén and Casey, 1996). The metal-organic bonding in the surface chelate formed with this bidentate ligand is very similar to that in the soluble Fe(III) chelate, which is a five-membered ring including the N-O bond (Holmén et al., 1997). No evidence for multinuclear surface complexes or unidentate ligation under the conditions of their experiments was found by Holmén et al. (1997). Holmén and Casey (1996; 1998) noted also that the adsorption envelope (graph of amount adsorbed versus pH) for acetohydroxamic acid on goethite was ligand-like (Stumm, 1992), as expected. The rate of goethite dissolution was much less than the rate of surface complex formation, leading therefore to the well-known linear correlation between the dissolution rate coefficient and adsorbed ligand concentration (Stumm et al., 1990).

In this paper, we report the first adsorption and dissolution experiments involving goethite and the fungal siderophore, desferrioxamine B. One objective of our study was to provide basic information about the surface concentrations of this trihydroxamate siderophore and its influence on goethite dissolution kinetics. Adsorption and dissolution experiments also were performed with an acetyl derivative of desferrioxamine B, namely desferrioxamine D_1, in which the proton on the terminal amine group in desferrioxamine B is replaced by an acetyl

*Address reprint requests to S. M. Kraemer, University of California, Berkeley, 235 Hilgard Hall, Berkely, CA 94720, USA (skraemer@nature.berkeley.edu).
Present address: Riedelsberger Weg 42, D-95448 Bayreuth, Germany

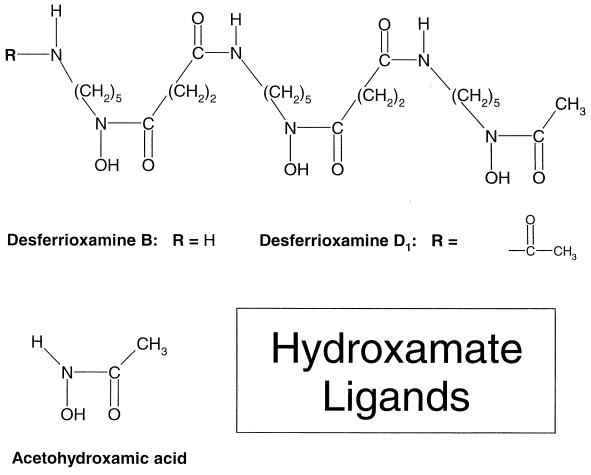

Fig. 1. Molecular structure of desferrioxamine B and D_1. The three hydroxamate groups are at the bottom of the structure. The small ligand, acetohydroxamic acid, shown at the lower left, contains only a single hydroxamate group.

group (Fig. 1), thereby removing a source of positive charge on the siderophore. Desferrioxamine B is a cationic species at pH $<$ 8 (Borgias et al., 1989). Desferrioxamine D_1 is excreted by the actinomycete *Streptomyces pilosus* (Bickel et al., 1960; van der Helm et al., 1987). It was used in our experiments to provide additional data for extrapolating from the behavior of the neutral acetohydroxamic acid (Holmén et al., 1997) to that of the positively-charged desferrioxamine B.

Although the stability constants of complexes between siderophores and other trace metals are not as high as that with Fe(III), they are not insignificant (Hernlem et al., 1995). These relatively high stability constants, together with the common occurrence of siderophores in soil environments, suggest that siderophores could potentially have impact on the transport and mobility of trace metals other than Fe(III). To explore this possibility, some of our experiments included adsorbed Pb(II) as a typical hazardous trace metal whose surface complexation reactions with goethite have been investigated extensively (e.g., Müller and Sigg, 1992; Rodda et al., 1993; Gunneriusson et al., 1994; Bargar et al., 1997), and for which formation constants of Pb(II)-desferrioxamine B complexes in aqueous solution are available (Hernlem et al., 1995). Our new results, pertaining to the effect of a hydroxamate siderophore on adsorbed Pb(II), are relevant to hazardous metal waste recovery and remediation in soils (Brainard et al., 1992).

2. EXPERIMENTAL

2.1. Materials

Goethite was synthesized by the method of Schwertmann and Cornell (1991) and freeze dried. Powder X-ray diffraction (Siemens) confirmed that the synthesized solid was goethite. Its specific surface area was 35 ± 3 m^2/g, as determined by the static BET method.

The sample of desferrioxamine B (DFO-B) used was produced by Ciba-Geigy (Desferal®) and received as a gift from the Salutar Corporation. The sample of desferrioxamine D1 (DFO-D1) used was prepared from DFO-B by per-acetylation in methanol. Hydrolysis of the hydroxamate esters of the per-acetylated DFO-B with ammonia gave the desired DFO-D1 product in good yield. The mesylate salt of DFO-B (6.58 g or 10 mmol) and sodium acetate (3.28 g or 40 mmol) were dissolved in 100 mL methanol. Acetic anydride (57 mL, 50 mmol) was added slowly to this ice-cooled solution. The mixture was stirred for 8 hr under N_2 and the volatile products were removed under vacuum. A colorless thick oil of per-acetylated DFO-B resulted and was used directly for the next step of the preparation reaction. The crude per-acetylated DFO-B was dissolved in methanol (40 mL) and diluted with diethyl ether (150 mL). After cooling at -20°C for 4 hr, the solution was filtered to remove insoluble material. The filtrate was saturated with gaseous ammonia and *N*-DFO-D1 was precipitated as a white solid, which was then washed with cold water (m.p. (uncorrected) 180–181°C). The product yield was 4.5 g (7.46 mmol, or 74.6%). A 500 MHz 1H NMR spectrum obtained on a Bruker AMX-500 spectrometer confirmed the composition and purity. Product analysis found calculated (measured) concentrations of $C_{27}H_{50}N_6O_9$ to be 53.82% (53.55%), 8.30% (8.40%), 13.95 (13.97%).

Solutions containing desferrioxamine B mesylate, desferrioxamine D_1, Pb ICP standard solution (Ultra Scientific), Fe ICP standard solution (Ultra Scientific), Na perchlorate (GFS, ACS grade), HEPES buffer [4-(2-hydroxyethyl)-1-piperazineethanesulfonic acid] (Sigma, Ultra), MOPS buffer (4-morpholinepropanesulfonic acid; Boehringer, reagent grade), Fe (III) perchlorate hexahydrate (GFS, ACS grade), perchloric acid (Fisher, Optima) were prepared with high-purity 18 MΩ cm^{-1} water (Milli-Q Plus, Millipore).

2.2. Analytical Methods

The concentrations of DFO-B and DFO-D1 were measured with a Shimadzu UV-160 spectrophotometer at 463.2 nm as the siderophore complex in the presence of excess Fe. To prevent precipitation of Fe hydroxide, the pH value was adjusted to 1.5 by adding a predetermined volume of perchloric acid (dilution effects taken into account). After acidification, Fe(III) perchlorate solution was added to a final Fe concentration of 312 μM. Standards were prepared with siderophore concentrations of 20, 40, 80, 120, 160, and 200 μM. Experimental samples were treated analogously to the standards. Iron and Pb were determined by ICP-AES (Thermo Jarrel-Ash) using emission lines at 238.2 and 220.3 nm, respectively. Proton activity was measured with a pH meter (Orion 720 A) and a Ross combination electrode calibrated with buffers at pH 4.0, 7.0, and 10.

2.3. Adsorption Measurements

Lead adsorption edge measurements (amount adsorbed as a function of pH) were performed in 0.01 M $NaClO_4$ at a goethite concentration of 0.5 g/L, open to the atmosphere, and at ambient temperature. Some samples contained 5 mM HEPES buffer. All samples were prepared in duplicate. Blanks (i.e., without goethite) were prepared over the pH range 3–9 to investigate Pb adsorption to container walls and filters, which was found to be $<$3% of the initial Pb concentration. In the batch adsorption experiments, 15 mg goethite and 25 g electrolyte (with or without buffer) were placed in 30 mL amber HDPE (high density poly (ethylene)) bottles. Lead and DFO-B stock solutions were added to final concentrations of 3.38 μM and 240 μM, respectively (Table 1). Predetermined amounts of acid or base were then added to reach the desired pH value for each sample. The sample bottle was filled with electrolyte (buffer) to a final mass of 30 g and placed on a rotary shaker for 18 h. The equilibrated samples were filtered using a 0.05 μm mixed cellulose acetate syringe filter (MF-Millipore). The first 3 mL of the filtrate were discarded, then 10 mL were filtered and retained for pH determination. Finally, 10 mL were collected for Pb and Fe analysis and acidified using 60 μL concentrated $HClO_4$. The saturation state of all relevant solid Pb hydroxides and carbonates were calculated, and it was ascertained that all such solid phases were undersaturated under the experimental conditions of our study.

Adsorption isotherms and envelopes for DFO-B and DFO-D1 on goethite were measured at a high solids concentration of 13 g/L, because preliminary experiments indicated that the maximum DFO-B and DFO-D1 surface concentrations on goethite are relatively low. A disadvantage of this arrangement is a high rate of iron dissolution and the concomitant decrease of the free ligand concentration, particularly in the presence of DFO-D1. Therefore, the reaction times were short: only 50 min for DFO-D1 and 18 hr for DFO-B. All adsorption measurements were performed in 0.01 M $NaClO_4$ solution with 5 mM

Table 1. Experimental conditions for adsorption and dissolution studies.

Experiment	Pb_{total} [μM]	$Ligand_{total}$ [μM]	pH	Solid/liquid [g/L]	Reaction time
Lead adsorption edge	3.48	None	3.5–7.5	0.5	18 h
	3.48	240 (DFO-B)	3.5–9.0	0.5	18 h
	3.48	240 (DFO-D1)	3.5–9.0	0.5	18 h
DFO-B adsorption isotherm	none	15–150	6.6	13	18 h
DFO-B adsorption envelope	none	150	3–9	13	18 h
DFO-D1 adsorption isotherm	none	10–150	6.6	13	50 min
DFO-D1 adsorption envelope	none	150	3.8–8.5	13	50 min
Dissolution kinetics	none	240 (DFO-B)	6.5	0.5	14.5 days
	none	240 (DFO-D1)	6.5	0.5	14.5 days
	3.48	240 (DFO-B)	6.5	0.5	14.5 days
	17.4	240 (DFO-B)	6.5	0.5	14.5 days
Dissolution kinetics (without pH buffer)	none	240 (DFO-B)	6.5	0.5	14.5 days

MOPS buffer, open to the atmosphere, and at ambient tempreature. All samples were prepared in duplicate. Blanks (i.e., without goethite) were prepared over the pH range 3–9 to investigate adsorption to container walls and filters, which was found to be <3.5% of the initial DFO-B or DFO-D1 concentration. In these batch studies, 390 mg goethite and 14 g electrolyte (with or without buffer) were placed in 30 mL amber HDPE bottles. Then DFO-B or DFO-D1 stock solution was added to give a final concentration of 150 μM for the adsorption edge determination and between 10 and 150 μM for the adsorption isotherm measurements (Table 1). Predetermined amounts of acid or base were added to reach the desired pH for each sample (i.e., pH 6.6 for the adsorption isotherm and pH 3 to 9 for the edge measurements). The sample bottle was filled with electrolyte solution to a final mass of 30 g and placed on a rotary shaker for 18 hr (DFO-B) or 50 min (DFO-D1) to minimize goethite dissolution. The samples were filtered using a 0.05 μM syringe filter (MF-Millipore). The first 3 mL of the filtrate were discarded, then 10 mL were filtered for pH measurement. Finally, 10 mL were collected for analysis of dissolved Fe and ligand concentrations.

2.4. Dissolution Kinetics

Goethite dissolution kinetics were measured at pH 6.5 (where proton and hydroxide effects on dissolution should be minimal and coagulation processes are negligible) in batch experiments with a solids concentration of 0.5 g/L in 0.01 M $NaClO_4$ solution. All samples contained 5 mM MOPS pH buffer except for one batch experiment that was performed to verify that this buffer does not influence goethite dissolution rates. Dissolution experiments in the presence of DFO and Pb were designed to investigate the effect of adsorbed Pb on dissolution. In each experiment, goethite was suspended in electrolyte solution by ultrasonification for 1 min. Then DFO-B (or DFO-D1) and Pb stock solutions were added (Table 1) and pH was adjusted to 6.5 with 0.1 M NaOH. Finally, electrolyte was added to make a final sample mass of 200 g. The samples then were continuously mixed on a horizontal shaker. Aliquots were taken over time and filtered with 0.05 μm syringe filters (MF-Millipore). The filtrate was acidified to approximately pH 1 with concentrated perchloric acid and stored in a refrigerator for no more than 1 wk prior to chemical analysis.

2.5. Data Treatment

Lead speciation in the presence of DFO-B was calculated using the chemical equilibrium model PHREEQC (Parkhurst, 1995). Thermodynamic constants used in the calculations were taken from the literature (Table 2). Since the Pb adsorption experiments were open to the atmosphere, the stability of Pb hydroxides and carbonates were calculated, and it was ascertained that all such solid phases were undersaturated under the experimental conditions of our study.

3. RESULTS

3.1. Adsorption of Lead

In the absence of an organic ligand, Pb is known to adsorb strongly to goethite with increasing pH (Hayes and Leckie, 1986; Roe et al., 1991; Müller and Sigg, 1992; Kooner, 1993; Rodda et al., 1993; Gunneriusson et al., 1994). Figure 2 (square symbols) indicates that $pH_{50} \approx 5.5$ and, at pH > 7, all Pb added is adsorbed. This result is consistent with previous observations of Pb adsorption, in the presence of a variety of background electrolytes at various initial Pb concentrations and solid concentrations. Both DFO-B and DFO-D1 similarly influence the adsorption of Pb above pH_{50} (Fig. 2). In the presence of

Table 2. Conditional formation constants (K_c) included in the model calculatons. All constants are corrected to I = 0.01 M.

Reaction	log K_c	Reaction	log K_c
$DFO^{3-} + H \Leftrightarrow HDFO^{2-}$	10.46[a]	$Pb^{2+} + OH^- + CO_3^{2-} \Leftrightarrow PbOH(CO_3)^-$	10.70[a]
$HDFO^{2-} + H^+ \Leftrightarrow H_2DFO^-$	9.35[a]	$Pb^{2+} + OH^- \Leftrightarrow PbOH^+$	6.58[a]
$H_2DFO^- + H^+ \Leftrightarrow H_3DFO$	8.90[a]	$Pb^{2+} + 2\ OH^- \Leftrightarrow Pb(OH)_{2(aq)}$	11.18[a]
$H_3DFO + H^+ \Leftrightarrow H_4DFO^+$	8.38[a]	$Pb^{2+} + 3\ OH^- \Leftrightarrow Pb(OH)_3^-$	14.23[a]
$Pb^{2+} + HDFO^{2-} \Leftrightarrow PbHDFO$	9.48[b]	$2\ Pb^{2+} + OH^- \Leftrightarrow Pb_2OH^{3+}$	7.61[a]
$Pb^{2+} + H_2DFO^- \Leftrightarrow PbH_2DFO+$	8.99[b]	$3\ Pb^{2+} + 4\ OH^- \Leftrightarrow Pb_3(HO)_4^{2+}$	32.66[a]
$Pb^{2+} + H_3DFO \Leftrightarrow PbH_3DFO^{2+}$	5.92[b]	$4\ Pb^{2+} + 4\ OH^- \Leftrightarrow Pb_4(HO)_4^{4+}$	36.20[a]
$2\ Pb^{2+} + HDFO^{2-} \Leftrightarrow Pb_2HDFO^{2+}$	15.77[b]	$6\ Pb^{2+} + 8\ OH^- \Leftrightarrow Pb_6(OH)_8^{4+}$	69.16[a]
$Pb^{2+} + CO_3^{2-} \Leftrightarrow PbCO_{3(aq)}$	4.56[a]	$H^+ + CO_3^{2-} \Leftrightarrow HCO_3^-$	10.46[a]
$Pb^{2+} + 2\ CO_3^{2-} \Leftrightarrow Pb(CO_3)_2^{2+}$	8.02[a]	$H^+ + HCO_3^- \Leftrightarrow H_2CO_3$	6.402[a]
$Pb^{2+} + CO_3^{2-} \Leftrightarrow PbCO_{3(s,Cerrusite)}$	−13.49[a]		

[a] Martell et al. (19995).
[b] Hernlem et al. (1995).

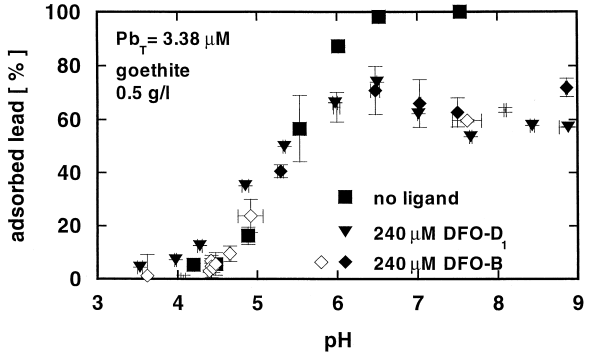

Fig. 2. Adsorption edge for Pb (initial conc. 3.38 μM) on goethite in the absence of siderophore, and in the presence of 240 μM DFO-B or DFO-D1. Error bars indicate twice the standard deviation of duplicate-sample measurements. Open diamonds are results obtained in the absence of pH-buffer; otherwise [HEPES] = 5 mM.

240 μM siderophore, adsorbed Pb does not exceed 70% of the initial concentration, an effect that can be understood qualitatively by considering the competition between goethite surface sites and siderophore ligands for Pb.

3.2. Adsorption of DFO-B and DFO-D1

Adsorption isotherms for DFO-B and DFO-D$_1$ at pH 6.6 are presented in Fig. 3. These L-type isotherms (Sposito, 1989) show maximum adsorbed siderophore concentrations of approximately 1.5 (DFO-B) and 3.5 (DFO-D1) μmol/g. Both of these surface concentrations are much smaller than even the lower range of previously-measured goethite surface-site concentrations (Cornell and Schwertmann, 1996). The adsorption envelope of DFO-D$_1$ (Fig. 4) is typical of a ligand (Stumm et al., 1990; Stumm, 1992), with maximum adsorption being observed at pH 4.2. By contrast, the adsorption envelope of DFO-B (Fig. 4) is more like that of a monovalent cation (Stumm et al., 1990; Stumm, 1992), with adsorbed concentrations close to 1.5 μmol/g achieved at pH < 7. Above pH 7.5, DFO-B adsorption increases to about 2.5 μmol/g.

3.3. Dissolution of Goethite

Figure 5 shows data on the dissolution of goethite in the presence of DFO-B or DFO-D1 at pH 6.5 and a total siderophore concentration of 240 μM. After an initial fast reaction, slow dissolution with a constant rate is observed. The dissolution rate in the presence of DFO-D1 (0.17 μmol/g $\cdot$ h) was almost an order of magnitude higher than the dissolution rate in the presence of DFO-B (0.02 μmol/g $\cdot$ h). This latter result is comparable with the dissolution rate of goethite (0.01 μmol/g $\cdot$ h) observed by Watteau and Berthelin (1994) at a lower total DFO-B concentration of 126 μM. The presence of adsorbed Pb (total added concentrations of 3.48 and 17.4 μM) had no significant effect on dissolution in the presence of DFO-B (Fig. 5). The dissolution rate in the absence of the pH buffer was similar to the rate in the presence of 5 mM MOPS, where solution pH drifted from 6.5 to 5.8.)

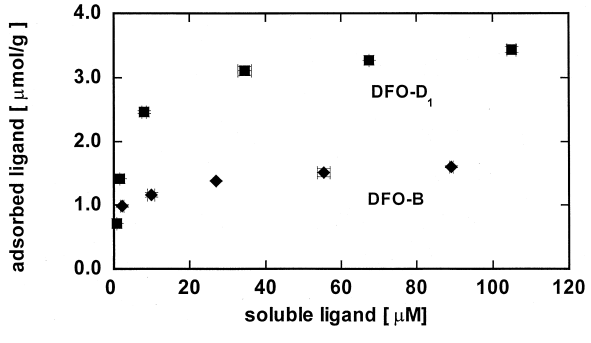

Fig. 3. Adsorption isotherms for DFO-B (diamonds) and DFO-D1 (squares) on goethite. Error bars indicate twice the standard deviation of duplicate-sample measurements: 0.01 M $NaClO_4$; solid conc. 13 g/L; [MOPS] = 5 mM; pH = 6.6.

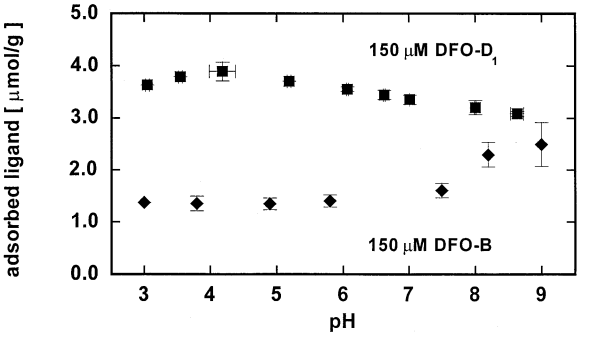

Fig. 4. Adsorption envelope for DFO-B (diamonds) and DFO-D$_1$ (squares) on goethite. Error bars indicate twice the standard deviation of duplicate-sample measurements. The total ligand concentration was 150 μM; 0.01 M $NaClO_4$; solid conc. 13 g/L; [MOPS] = 5 mM.

4. DISCUSSION

At pH > 5.5, a significant effect of DFO-B and DFO-D$_1$ on the adsorption of Pb by goethite was found at the initial Pb/siderophore molar ratio of 0.014 used in this study (Fig. 2). It is noteworthy that, under the conditions of the present experiments, DFO-B and DFO-D$_1$ were able to mobilize about

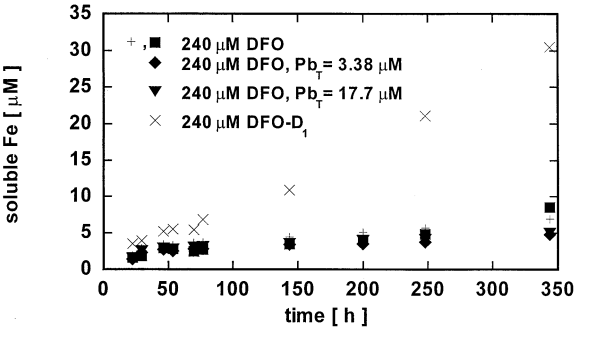

Fig. 5. Iron release by goethite in the presence of DFO-D$_1$ (X) or DFO-B (all other symbols). The effect of Pb on DFO-B-promoted dissolution was investigated by adding total Pb at concentrations of 3.38 or 17.7 μM (diamond and triangle, respectively). The pH was 6.5 with a buffer concentration of 5 mM (MOPS), except for one series of experiments (+) that was performed without buffer and in which pH was allowed to drift from pH 6.5 initially to 5.8. The ligand concentration was 240 M in all experiments; 0.01 M $NaClO_4$; solid conc. 0.5 g/L.

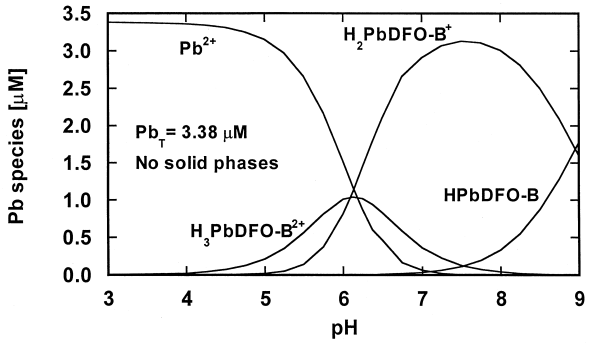

Fig. 6. Calculated speciation of 3.38 M Pb(II) in the presence of 240 M DFO-B but in the absence of solid phases (Martell et al., 1995; Hernlem et al., 1995). Note the peak for the complex H_2PbDFO^+ just below pH 8.

one-third of the Pb adsorbed on goethite at pH $>$ 6.5. In the case of DFO-B, the suppression of Pb adsorption was greatest just below pH 8, where the soluble complex species H_2PbDFO^+ has its maximum concentration (Fig. 6). In the case of DFO-D1, the absence of any increase in Pb adsorption at pH $>$ 8 could reflect the absence of positively charged soluble Pb species that can be attracted to the goethite surface.

The low adsorption capacity of goethite for DFO-D1 at pH 4 (4 μmol/g, Fig. 4) suggests that the binding of the siderophore at the mineral surface is limited by stereochemical constraints. Under our experimental conditions (pH 6.6), the maximum surface concentration of DFO-D1 is about 3.5 μmol/g (Fig. 3). This result can be compared directly with the surface concentration of acetohydroxamic acid (aHA) measured on goethite under comparable conditions by (Holmén and Casey, 1996), 10 μmol/g. Iron(III) coordination by aHA has been investigated by CIR-FTIR spectroscopy (Holmén et al., 1997), which shows that this bidentate ligand forms only mononuclear complexes both in solution and at the goethite surface. If excess ligand is present (i.e., $L_{diss}/Fe_{diss} > 3$), $Fe(aHA)_3$ is the dominant solution complex near neutral pH (Holmén and Casey, 1996) with a formation constant of $10^{28.3}$ (Martell et al., 1995). Compared to the dissolved tris aHA complex, Fe(III) complexation by DFO-B or DFO-D1 in solution exhibits only a small chelate effect, with a Fe(III) complex formation constant of 10^{31} (Albrecht-Gary and Crumbliss, 1998). This suggests that the three ligating groups, connected by a flexible linear organic chain (Fig. 1), coordinate Fe(III) in solution independently, in effect-like, coordination by three discrete aHA ligands. If similar behavior occurs at low surface coverage on goethite, a ratio of adsorbed DFO-D1 to aHA equal to 1/3, as described above, is indeed expected under similar experimental conditions. The maximum DFO-B surface concentration, on the other hand, is less than half that of DFO-D1 (Fig. 4). Since the coordinating groups of the 2 ligands are identical, the difference in adsorption behavior must arise from a difference in molecular species charge. The positive charge on DFO-B leads to electrostatic repulsion between the ligand and the goethite surface, which is also positively charged for pH $<$ 8. At pH $>$ 8, electrostatic repulsion no longer exists and the adsorbed concentrations of DFO-B and DFO-D1 indeed do converge (Fig. 4).

Our goethite dissolution experiments in the presence of DFO-B or DFO-D1 were conducted at pH 6.5 with a total ligand concentration of 240 μM. The dissolution rate in the presence of DFO-D1 (0.17 μmol/g $\cdot$ h) is in good agreement with that reported by Holmén and Casey (1998) for goethite in the presence of aHA at a surface concentration of 10 μmol/g (i.e., at 3 times the DFO-D1 surface concentration), which is 0.16 μmol/g $\cdot$ h (Holmén and Casey, 1998). The surface concentration of DFO-D1 is about twice that of DFO-B under these conditions (Fig. 3), but the dissolution rate in the presence of DFO-D1 is more than 8 times higher than in the presence of DFO-B. Hence, the effect of these two ligands on the goethite dissolution rate is not linearly related to the adsorbed coordinating-ligand concentration.

Acknowledgments—This research was supported in part by the Director, Office of Energy Research, Office of Basic Energy Sciences, Geosciences Program, of the US Department of Energy under Grant No DE-FG03-96ER14667. Thanks to Brian Schroth for technical assistance and for insightful discussions. Gratitude is expressed to Angela Zabel for preparation of the typescript.

REFERENCES

Albrecht-Gary A.-M. and Crumbliss A. L. (1998) Coordination chemistry of siderophores: Thermodynamics and kinetics of iron chelation and release. *Metal Ions Biol. Sys.* **35,** 239–327.

Bargar J. R., Brown G. E., and Parks G. A. (1997) Surface complexation of Pb(II) at oxide-water interfaces: II. XAFS and bond-valence determination of mononuclear Pb(II) sorption products and surface functional groups on oxides. *Geochim. Cosmochim. Acta* **61,** 2639–2652.

Bickel H., Bosshardt R., Gaeumann E., Reusser P., Vischer E., Voser W., Wettstien A., and Zaehner H. (1960) Ueber die Isolierung und Charakterisierung der Ferrioxamine A-F, neuer Wuchsstoffe der Sideramin-Gruppe. *Helv. Chim. Acta* **43,** 2118–2128.

Borgias B., Hugi A. D., and Raymond K. N. (1989) Isomerization and solution structures of desferrioxamine B complexes of Al^{3+} and Ga^{3+}. *Inorg. Chem.* **28,** 3538–3545.

Brainard J. R., Strietelmeier B. A., Smith p. H., Langston-Unkefer P. J., Barr M. E., and Ryan R. R. (1992) Actinide binding and solublization by microbial siderophores. *Radiochim. Acta* **58/59,** 357–363.

Cornell R. M. and Schwertmann U. (1996) *The Iron Oxides*. VCH.

Crowley D. E. and Gries D. (1994) Modeling of iron availability in the plant rhizosphere. In *Biochemistry of Metal Micronutrients in the Rhizosphere* (ed. J.A. Manthey, D.E.Crowley, and D.G. Luster), pp. 199–223. CRC Press, Boca Raton, FL.

Crowley D. E., Reid C. P. P., and Szaniszlo P. J. (1987) Microbial siderophores as iron sources for plants. In *Iron Transport in Animals, Plants, and Microorganisms* (eds. G. Winkelmann, D. van der Helm, and J. B. Neilands), pp. 375–385. VCH Publishers, Mannheim, Germany.

Dzombak D. A. and Morel F. M. M. (1990) *Surface Complexation Modeling.* John Wiley.

Gunneriusson L., Lövgren L., and Sjöberg S. (1994) Complexation of Pb(II) at the goethite (αFeOOH)/water interface: The influence of chloride. *Geochim. Cosmochim. Acta* **58,** 4973–4983.

Hayes K. F. and Leckie J. O. (1986) Mechanism of lead ion adsorption at the goethite-water interface. In *Geochemical Processes at Mineral Surfaces* (ed. J. A. Davis and K. F. Hayes), Vol. 323, pp. 114–141. ACS symposium series.

Hernlem B. J., Vane L. M., and Sayles G. D. (1995) Stability constants for complexes of the siderophore desferrioxamine B with selected heavy metal cations. *Inorg. Chim. Acta* **244,** 179–184.

Holmén B. A. and Casey W. H. (1996, 1998) Hydroxamate ligands, surface chemistry, and the mechanism of ligand-promoted dissolution of goethite [-FeOOH(s)]. *Geochim. Cosmochim. Acta* **60,** 4403–4416; *Ibid.* **62,** 726.

Holmén B. A., Tejedor-Tejedor M. I., and Casey W. H. (1997) Hydroxamate complexes in solution and at the goethite-water interface:

A cylindrical internal reflection Fourier transform infrared spectroscopy study. *Langmuir* **13,** 2197–2206.

Kooner Z. S. (1993) Comparative study of adsorption behavior of copper, lead, and zinc onto goethite in aqueous systems. *Environ. Geol.* **21,** 242–250.

Martell A. E., Smith R. M., and Motekaitis R. J. (1995) *Critical Stability Constants Database*. NIST., Vol. 2.

Müller A. and Sigg L. (1992) Adsorption of Lead(II) on the goethite surface: Voltammetric evaluation of surface complexation parameters. *J. Colloid Interface Sci.* **148,** 517–532.

Parkhurst D. L. (1995) User's guide to PHREEQC-A computer program for speciation, reaction-path, advective-transport, and inverse geochemical calculations. *USGS Water Resources Investigations Report 95-4227.*

Powell, P. E., Szaniszlo P. J., Cline G. R., and Reid C. P. P. (1982) Hydroxamate siderophores in the iron nutrition of plants. *J. Plant Nutr.* **5,** 653–673.

Rodda D. P., Johnson B. B., and Wells J. D. (1993) The effect of temperature and pH on the adsorption of copper(I), lead(II), and zinc(II) onto goethite. *J. Colloid Interface Sci.* **161,** 57–62.

Roe A. L., Hayes K. F., Chisholm-Brause C., Brown G. E., Parks G. A., Hodgson K. O., and Leckie J. O. (1991) In situ X-ray adsorption study of lead ion surface complexes at the goethite-water interface. *Langmuir* **7,** 367–373.

Schwertmann U. and Cornell R. M. (1991) *Iron Oxides in the Laboratory.* VCH Publishers.

Sposito G. (1989) *The Chemistry of Soils.* Oxford University Press.

Stumm W. (1992) *Chemistry of the Solid-Water Interface*. Wiley-Interscience.

Stumm W., Suzberger B., and Sinniger J. (1990) The coordination chemistry of the oxide-electrolyte interface: The dependence of surface reactivity (dissolution, redox reactions) on surface structure. *Croat. Chem. Acta* **63,** 277–312.

Telford J. R. and Raymond K. N. (1996) Siderophores. In *Comprehensive Supramolecular Chemistry* (ed. J. L. Atwood, J. E. D. Davies, D. D. MacNicol, and F. Vogtle), Vol. 10, pp. 537–555. Elsevier Science.

van der Helm, D., Jalal, M. A. F., and Hossain, M. B. (1987) The crystal structures, conformations, and configurations of siderophores. In *Iron Transport in Microbes, Plants and Animals* (eds. G. Winkelmann, D. van der Helm, and J. B. Neilands), pp. 135–165. VCH Publishers, Mannheim, Germany.

Watteau F. and Berthelin J. (1994) Microbial dissolution of iron and aluminium from soil minerals: Efficiency and specificity of hydroxamate siderophores compared to aliphatic acids. *Eur. J. Soil Biol.* **30,** 1–9.